Steel and Composite Structures, Vol. 1, No. 1 (2001) 51-74
DOI: http://dx.doi.org/10.12989/scs.2001.1.1.051

Tests and mechanics model for concrete-filled SHS stub columns, columns and beam-columns

Lin-Hai Han†

College of Civil Engineering and Architecture, Fuzhou University, Gongye Road 523, Fuzhou, Fujian Province, 350002, China

Xiao-Ling Zhao‡

Department of Civil Engineering, Monash University, Clayton, VIC 3168, Australia

Zhong Tao‡

College of Civil Engineering and Architecture, Fuzhou University, Gongye Road 523, Fuzhou, Fujian Province, 350002, China

Abstract. A series of tests on concrete-filled SHS (Square Hollow Section) stub columns (twenty), columns (eight) and beam-columns (twenty one) were carried out. The main parameters varied in the tests are (1) Confinement factor (ξ) from 1.08 to 5.64, (2) concrete compression strength from 10.7 MPa to 36.6 MPa, (3) tube width to thickness ratio from 20.5 to 36.5. (4) load eccentricity (e) from 15 mm to 80 mm and (5) column slenderness (λ) from 45 to 75. A mechanics model is developed in this paper for concrete-filled SHS stub columns, columns and beam-columns. A unified theory is described where a confinement factor (ξ) is introduced to describe the composite action between the steel tube and filled concrete. The predicted load versus axial strain relationship is in good agreement with stub column test results. Simplified models are derived for section capacities and modulus in different stages of the composite sections. The predicted beam-column strength is compared with that of 331 beam-column tests with a wide range of parameters. A good agreement is obtained. The predicted load versus mid-span deflection relationship for beam-columns is in good agreement with test results. A simplified model is developed for calculating the member capacity of concrete-filled SHS columns. Comparisons are made with predicted columns strengths using the existing codes such as LRFD (AISC 1994), AIJ (1997), and EC4 (1996). Simplified interaction curves are derived for concrete-filled beam-columns.

Key words: composite actions; concrete-filled tubes; mechanics model; steel hollow sections; stub columns; columns; beam-columns; constraining factor; section capacity; member capacity.

1. Introduction

Steel tubular sections (circular or square) filled with concrete are widely used in building construction (ASCCS 1997, Bergmann *et al*. 1995, Shams and Saadeghvaziri 1997). The composite

†Professor
‡Ph.D.

tubular columns have better structural performance than that of bare steel or bare concrete. Steel hollow section acts as casting as well as reinforcement for the concrete (Bergmann *et al.* 1995). Concrete eliminates or delays the local buckling of steel hollow sections, and increases significantly the ductility of the section (Bridge *et al.* 1995, O'Shea and Bridge 1997, Nakai *et al.* 1994, Ge and Usami 1992, 1996, Schneider 1998, Kitada 1998, Uy 1998, Zhao and Grzebieta 1999, Zhao *et al.* 1999, Han 2000).

Simple superposition of the strength of concrete and steel tubes was used traditionally to estimate the section capacity of concrete-filled SHS stub columns (Nakai *et al.* 1986, Liu and Goel 1988, Bergmann *et al.* 1995). Simple superposition tends to give reasonable estimation of ultimate section capacity but underestimate the ductility of the composite section. An efficient ductility of composite sections is very important especially under earthquake loading. The interaction between steel tube and concrete is the key issue to understand the behaviour of concrete-filled tubular members. This paper address concrete-filled Square Hollow Section (SHS) stub columns, columns and beam-columns.

The mechanical properties of confined concrete by transverse steel reinforcement have been reported by Mander *et al.* (1988a, 1988b), Trezona and Warner (1997). Finite element analysis has been carried out recently to study the axially loaded concrete-filled steel tubes (Schneider 1998, Ge and Usami 1994).

This paper develops a mechanics model that can predict the behaviour of concrete filled SHS stub columns in compression. A unified theory (Han 1998) is described where a confinement factor (ξ) is introduced to describe the composite action between the steel tube and filled concrete. Twenty stub column tests were carried out in compression. The main parameters varied in the tests are (1) confinement factor (ξ) from 1.08 to 5.64, (2) concrete compression strength from 10.7 MPa to 36.6 MPa, (3) tube width to thickness ratio from 20.5 to 36.5. The load versus axial strain relationship is established for concrete-filled SHS stub columns both experimentally and theoretically. The predicted curves of load versus axial strain are in good agreement with test results. Simplified models are derived for section capacities, modulus in different stages (elastic, inelastic and strain hardening) of composite sections.

Tests on 8 columns and 21 beam-columns were carried out too. The main parameters varied in the tests are: (1) Confinement factor (ξ), from 1.08 to 3.27; (2) Concrete compression strength, from 18.8 MPa to 36.6 MPa; (3) Tube width to thickness ratio, from 20.5 to 36.5; (4) Load eccentricity (e), from 15 mm to 80 mm; (5) Column slenderness (λ), from 45 to 75. A mechanics model is developed for concrete-filled SHS (Square Hollow Section) columns and beam-columns. The unified theory mentioned above is adopted where the confinement factor (ξ) is used. The predicted column strength is compared with that of 331 column tests with a wide range of parameters such as the confinement factor (ξ), the slenderness ratio (λ), the concrete strength (f_{ck}), the steel yield stress (f_{sy}) and the load eccentricities (e). Good agreement was obtained. The load versus mid-span deflection relationship is established for concrete-filled SHS beam-columns both experimentally and theoretically. The predicted curves of load versus mid-span deflection are in good agreement with test results. A simplified model is developed for calculating the member capacity of concrete-filled SHS columns. Simplified interaction curves are derived for concrete-filled beam-columns. Comparisons are made with predicted column strengths using LRFD (AISC 1994), AIJ (1997) and EC4 (1996).

2. Experimental investigation

The aim of the experimental study was to determine not only the maximum load capacity of the

Table 1 Specimen labels, material properties, section capacities and ductility index (stub columns)

Specimen Label	$B\times t$ (mm)	f_{sy} (MPa)	f_{ck} (MPa)	ξ	$N_{u,e}$ (kN)	$N_{u,c}$ (kN)	$N_{u,e}/N_{u,c}$	DI
sczs1-1-1	120×3.84	330	18.29	2.55	882	894	0.987	2.4
sczs1-1-2	120×3.84	330	20.92	2.23	882	934	0.944	2.0
sczs1-1-3	120×3.84	330	20.92	2.23	921	934	0.986	1.5
sczs1-1-4	120×3.84	330	33.01	1.41	1080	1115	0.969	2.6
sczs1-1-5	120×3.84	330	35.23	1.33	1078	1148	0.939	2.6
sczs1-2-1	140×3.84	330	10.65	3.52	941	945	0.996	>14.3
sczs1-2-2	140×3.84	330	11.21	3.34	922	958	0.962	7.8
sczs1-2-3	140×3.84	330	36.60	1.08	1499	1489	1.007	2.2
sczs1-2-4	140×3.84	330	36.60	1.08	1470	1489	0.987	1.7
sczs2-1-1	120×5.86	321	20.07	3.65	1176	1172	1.003	>8.4
sczs2-1-2	120×5.86	321	20.07	3.65	1117	1172	0.953	>17
sczs2-1-3	120×5.86	321	17.25	4.25	1196	1129	1.059	13.3
sczs2-1-4	120×5.86	321	35.23	2.08	1460	1388	1.052	3.7
sczs2-1-5	120×5.86	321	35.23	2.08	1372	1388	0.988	3.0
sczs2-2-1	140×5.86	321	10.87	5.64	1343	1245	1.079	>14
sczs2-2-2	140×5.86	321	12.22	5.02	1292	1278	1.011	>14
sczs2-2-3	140×5.86	321	36.60	1.68	2009	1773	1.133	1.67
sczs2-2-4	140×5.86	321	36.60	1.68	1906	1773	1.075	2.28
sczs2-3-1	200×5.86	321	11.76	3.51	2058	2028	1.015	5
sczs2-3-2	200×5.86	321	11.76	3.51	1960	2028	0.966	6
Mean	--	--	--	--	--	--	1.006	--
COV	--	--	--	--	--	--	0.0491	--

specimens, but also to investigate the failure pattern up to and beyond the ultimate load.

Strips of the steel tubes were tested in tension in accordance with the Chinese standard related to mental materials. Three coupons were taken from each face of a SHS, from these tests, the average yield strength (f_{sy}) was found to be 325 MPa as shown in Table 1, and the modulus of elasticity was about 200,000 MPa.

Four types of concrete were used. For each batch of concrete mixed, three 100 mm cubes were also cast and cured in conditions similar to the related specimens. The composite columns were tested at an age of 28 days after concrete casting. The average compression cube strengths (f_{cu}) at that age were 16.22 MPa, 25.75 MPa, 32.33 MPa and 49.27 MPa respectively. The modulus of elasticity (E_c) of concrete was measured in accordance with the Chinese related to concrete, the average values being 25,600 MPa, 26,230 MPa, 26,344 MPa and 28,740 MPa respectively. The average compression strength (f_{ck}, the value of f_{ck} is determined using 67% of the compression strength of cubic blocks.) of the specimens at time of testing were listed in detail in Table 1 and Table 2.

The experimental program consisted of two phases which are described below respectively.

2.1. Short column tests

2.1.1. Specimens

A total of twenty specimens were tested. A summary of the specimens is presented in Table 1 where the section sizes, material properties and confinement factors (ξ) are given. The specimens

Table 2 Specimen labels, material properties and member capacities (columns and beam-columns)

Member Type	Specimen Label	$B\times t$ (mm)	λ	e (mm)	f_{sy} (MPa)	f_{ck} (MPa)	ξ	$N_{u,e}$ (kN)	$N_{u,c}$ (kN)	$N_{u,e}/N_{u,c}$
Column	scp2-1-1	120×5.86	75	0	321	25.46	3.11	1000	979	1.021
	scp2-3-1	200×5.86	45	0	321	20.96	1.97	2083	2193	0.950
	sczL-1-1	120×3.84	75	0	330	22.32	2.09	754	747	1.009
	sczL-1-2	120×3.84	75	0	330	22.32	2.09	833	747	1.115
	sczL-1-3	120×3.84	75	0	330	36.60	1.28	980	855	1.146
	sczL-2-1	140×3.84	64	0	330	22.17	1.78	1049	991	1.059
	sczL-2-2	140×3.84	64	0	330	22.17	1.78	1127	991	1.137
	sczL-2-3	140×3.84	64	0	330	36.60	1.08	1323	1164	1.137
Mean	--	--	--	--	--	--	--	--	--	1.072
COV	--	--	--	--	--	--	--	--	--	0.0682
Beam-column	scp1-1-1	120×3.84	75	15	330	18.93	2.47	588	519	1.133
	scp1-1-2	120×3.84	75	30	330	18.93	2.47	451	408	1.105
	scp1-1-3	120×3.84	75	40	330	25.46	1.83	421	385	1.094
	scp1-1-4	120×3.84	75	50	330	18.93	2.47	333	324	1.028
	scp1-1-5	120×3.84	75	40	330	25.46	1.83	418	385	1.086
	scp1-1-6	120×3.84	75	50	330	36.60	1.28	423	381	1.110
	scp1-2-1	140×3.84	64	15	330	23.55	1.67	833	762	1.093
	scp1-2-2	140×3.84	64	40	330	23.55	1.67	615	542	1.135
	scp1-2-3	140×3.84	64	60	330	23.55	1.67	510	447	1.141
	scp1-2-4	140×3.84	64	40	330	25.46	1.55	559	554	1.009
	scp1-2-5	140×3.84	64	60	330	36.60	1.08	539	509	1.059
	scp2-1-2	120×5.86	75	15	321	23.55	3.11	755	696	1.085
	scp2-1-3	120×5.86	75	30	321	23.55	3.11	549	548	1.002
	scp2-1-4	120×5.86	75	50	321	23.55	3.11	511	437	1.169
	scp2-2-1	140×5.86	64	15	321	19.22	3.14	1014	920	1.102
	scp2-2-2	140×5.86	64	30	321	19.22	3.14	804	740	1.086
	scp2-2-3	140×5.86	64	40	321	18.76	3.27	735	656	1.120
	scp2-2-4	140×5.86	64	60	321	18.76	3.27	556	544	1.022
	scp2-3-2	200×5.86	45	30	321	26.77	1.54	1793	1698	1.056
	scp2-3-3	200×5.86	45	50	321	22.79	1.81	1426	1337	1.067
	scp2-3-4	200×5.86	45	80	321	26.77	1.54	1201	1134	1.059
Mean	--	--	--	--	--	--	--	--	--	1.084
COV	--	--	--	--	--	--	--	--	--	0.0414

were so designed that a wide range of confinement factor (from 1.08 to 5.64) was achieved.

A limit ratio of overall depth to thickness (B/t) is given by Bergmann *et al*. (1995) for concrete-filled rectangular hollow sections to prevent local buckling, i.e.,

$$B/t \le 52 \cdot \sqrt{\frac{235}{f_{sy}}} \tag{1}$$

where, the units for the steel yield stress (f_{sy}) are N/mm^2.

The tube width to thickness ratio listed in Table 1 varied from 20.5 to 36.5, while the limit given

by the above equation is found to be around 44. A slightly larger value of B/t limit was given by O'shea and Bridge (1997) and Uy *et al*. (1998). It is therefore expected that the concrete filled SHS sections have certain ductility.

The length of stub columns (L) were chosen to be three times the width of SHS sections to avoid the effects of overall buckling and end conditions (SAA 1996, Zhao and Hancock 1991, Han 2000).

The ends of the steel tubes were cut and machined to the required length. The insides of the tubes were wire brushed to remove any rust and loose debris present. The deposits of grease and oil, if any, were cleaned away. Each tube was welded to a square steel base plate 25 mm thick. The concrete was filled in layers and was vibrated by a poker vibrator. The specimens were placed upright to air-dry until testing. During curing, a very small amount of longitudinal shrinkage of 0.5 mm or so occurred at the top of the column. A high-strength epoxy was used to fill this longitudinal gap so that the concrete surface was flush with the steel tube at the top.

Prior to testing, the top surfaces of the concrete filled steel tubes were ground smooth and flat using a grinding wheel with diamond cutters. This was to ensure that the load was applied evenly across the cross-section and simultaneously to the steel and concrete.

2.1.2. Test set up and measurements

All the tests were performed on a 5000 kN capacity testing machine. The specimens were placed into the testing machine and the loads were applied on the specimens directly. Eight strain gauges were used for each specimen to measure strains at the middle height. Two displacement transducers were used to measure the axial deformation. A typical set up is shown in Fig. 1(a).

A load interval of less than one tenth of the estimated load capacity was used. Each load interval was maintained for about 2 to 3 minutes. Fig. 1(b) gives a general view of the test arrangement. The loading ram is a solid steel plate which acts like an end stiffener as shown in Fig. 1(b).

2.1.3. Test results

Typical failure mode was local (outward folding) failure mechanism. This is the same as that

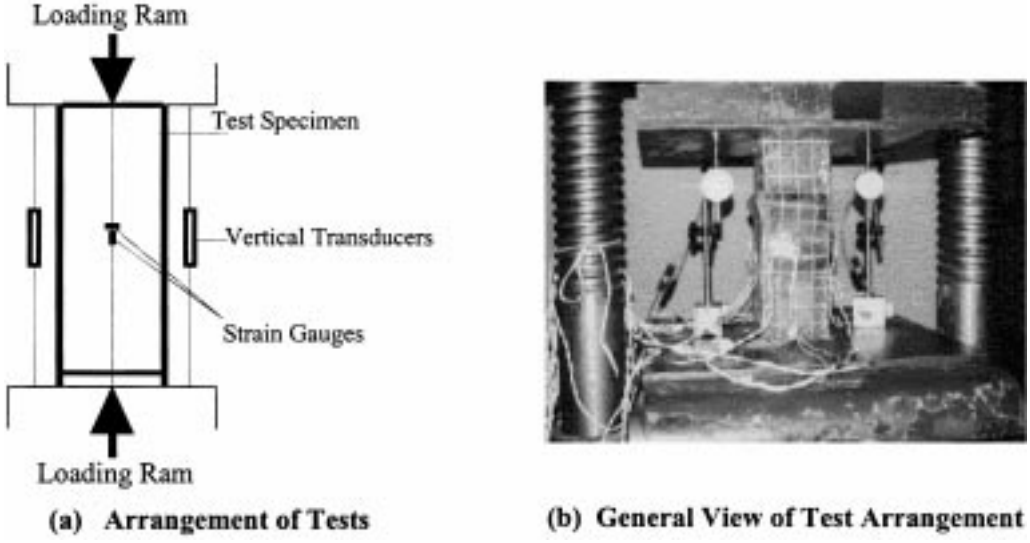

Fig. 1 Test set Up of the stub columns

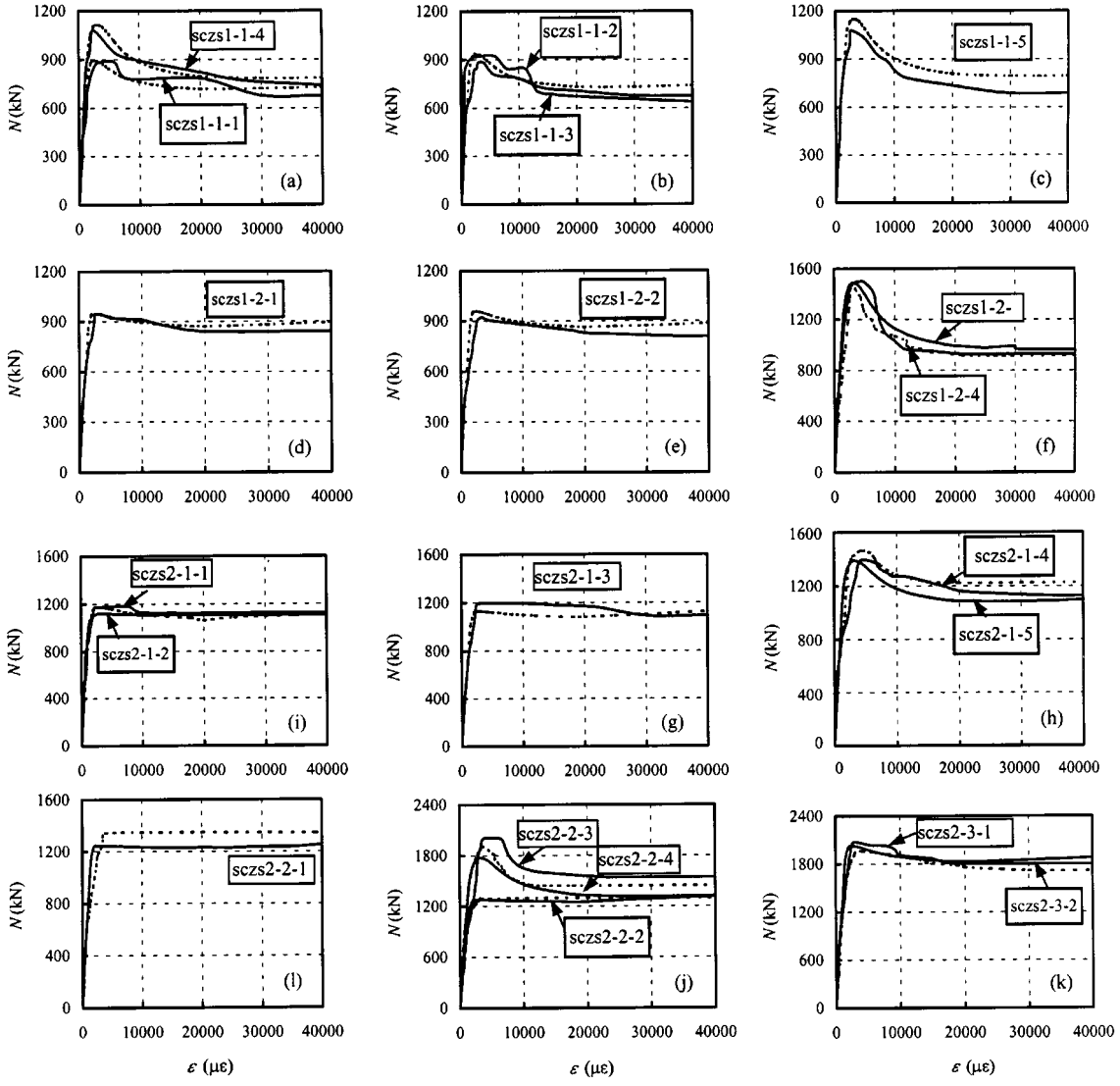

Fig. 2 Load versus axial strain curves(Experimental curves are shown in solid lines; Predicted curves are shown in dashed lines)

observed by many other researchers, such as Ge and Usami (1992), Zhao *et al.* (1999), O'shea and Bridge (1997), Song and Kwon (1997), Tomii and Sakino (1977) and etc. for concrete filled SHS sections. Total of the tested curves of load versus axial strain are shown in Fig. 2 in solid lines. It can be seen that the curves tend to drop quickly after the peak load for specimens with small confinement factor, whereas for larger confinement factors the load tends to maintain after the peak. The maximum loads ($N_{u,e}$) obtained in the test are summarised in Table 1.

2.1.4. Ductility index

One of the methods used to quantify section ductility is the ductility index (Murray 1986). Several

definitions of ductility index (DI) were used by various researchers based on load versus axial deformation curves (Zhao and Hancock 1991, Ge and Usami 1996) or load versus axial strain curves (Tao *et al*. 1998). The definition given in Tao *et al.* (1998) is adopted in this paper. It is expressed as:

$$DI = \frac{\varepsilon_{85\%}}{\varepsilon_u} \tag{2}$$

where ε_u is the strain at the ultimate load and $\varepsilon_{85\%}$ is the strain when the load falls to 85% of the ultimate load.

The ductility index so determined is listed in Table 1. They are plotted in Fig. 3 against the confinement factor (ξ) for the 20 specimens listed in Table 1. It can be seen from Fig. 3 that the ductility index increases rapidly when the confinement factor exceeds 3.5.

2.2. Column and beam-column tests

Eight tests on concentrically loaded composite columns were carried out. A total of 21 specimens were tested with eccentric loading. A summary of the specimens is presented in Table 1 where the section sizes, slenderness ratios (λ), load eccentricities (e), material properties (f_{sy} and f_{ck}) and confinement factors (ξ) are given. The parameter ranges are: (λ) from 45 to 75; e from 0 mm to 80 mm; f_{ck} from 18.8 MPa to 36.6 MPa and ξ from 1.08 to 3.27.

The specimens were fabricated like that stub columns. During concrete curing, a very small amount of longitudinal shrinkage of 1.0 to 1.3 mm or so occurred at the top of the column. A high-strength epoxy was used to fill this longitudinal gap so that the concrete surface was flush with the steel tube at the top.

Prior to testing, the top surfaces of the concrete filled steel tubes were ground smooth and flat using a grinding wheel with diamond cutters. This was to ensure that the load was applied evenly across the cross-section and simultaneously to the steel and concrete. The desired eccentricity was achieved by accurately machining grooves 6 mm deep into the stiff end plate that was welded together with the steel tubes. For the pure axial compression column, the groove was in the middle of the plate. The endplate was very stiff with a thickness of 30 mm. The axial load was applied through a very stiff top platen with an offset triangle hinge which also allowed specimen rotation. Both the endplate and the top platen were made of very hard and very high strength steel.

The value of slenderness ratio (λ) is defined as:

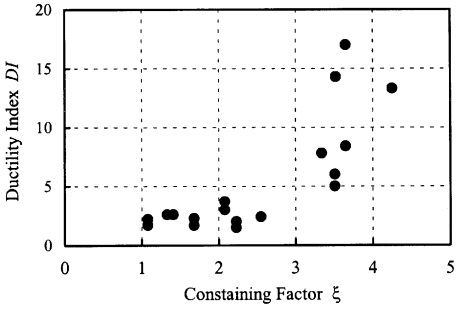

Fig. 3 Ductility index versus constraining factor

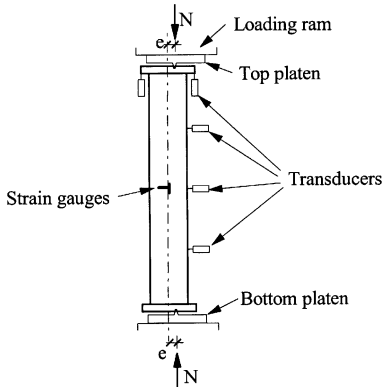

Fig. 4 Test set up of the columns and beam-columns

$$\lambda = \frac{L_e}{r}\sqrt{\frac{f_{sy}}{235}} \tag{3}$$

where L_e is the effective length of a column, which is the same as the physical length of the column (L) with pin-ended supports.

2.2.1. Test set up and measurements

All the tests were performed on a 5000 kN capacity testing machine. A typical setup is shown in Fig. 4. Eight strain gauges were used for each specimen to measure the longitudinal and transverse strains at the middle height. Two displacement transducers were used to measure the axial deformation. Three transducers were used to measure the lateral deflection. A load interval of less than one tenth of the estimated load capacity was used. Each load interval was maintained for about 2 to 3 minutes.

2.2.2. Test results

Typical failure mode was overall buckling failure. When the load was small, the lateral deflection at middle height is small and approximately proportional to the applied load. When the load reached about 60% to 70% of the maximum load, the lateral deflection at middle height started to increase significantly. Total of the tested curves of load versus lateral deflection (u_m) curves are shown in Fig. 5 in solid lines. The maximum loads ($N_{u,e}$) obtained in the test are summarised in Table 2.

3. Mechanics model for concrete-filled SHS stub columns

3.1. Material properties

A typical stress-strain curve for steel can consist of five stages as shown in Fig. 6. Detailed expressions are given in Pan (1988) as:

$$\sigma = E_s \cdot \varepsilon \qquad \text{for } \varepsilon \le \varepsilon_1 \tag{4a}$$

$$\sigma = -A \cdot \varepsilon^2 + B \cdot \varepsilon + C \qquad \text{for } \varepsilon_1 < \varepsilon \le \varepsilon_2 \tag{4b}$$

$$\sigma = f_{sy} \qquad \text{for } \varepsilon_2 < \varepsilon \le \varepsilon_3 \tag{4c}$$

$$\sigma = f_{sy} \cdot \left[1 + 0.6 \cdot \frac{\varepsilon - \varepsilon_3}{\varepsilon_4 - \varepsilon_3}\right] \qquad \text{for } \varepsilon_3 < \varepsilon \le \varepsilon_4 \tag{4d}$$

$$\sigma = 1.6 \cdot f_{sy} \qquad \text{for } \varepsilon > \varepsilon_4 \tag{4e}$$

where, E_s=200,000 MPa, $\varepsilon_1 = 0.8 \cdot f_{sy}/E_s$, $\varepsilon_2 = 1.5 \cdot \varepsilon_1$, $\varepsilon_3 = 10 \cdot \varepsilon_2$, $\varepsilon_4 = 100 \cdot \varepsilon_2$. f_{sy} is the yielding strength of the steel. In Fig. 6, $f_{sp} = 0.8\, f_{sy}$, $f_{su} = 1.6\, f_{sy}$.

A typical stress-strain curve for confined concrete is shown in Fig. 7 where the confinement factor (ξ) is defined as:

$$\xi = \frac{A_s \cdot f_{sy}}{A_c \cdot f_{ck}} \tag{5}$$

in which A_s is the cross-section area of steel tube, A_c is the cross-section area of concrete, f_{sy} is the yield stress of steel tube and f_{ck} is the compression strength of concrete. The value of f_{ck} is determined using 67% of the compression strength of cubic blocks. Detailed expressions are given in Tao *et al.* (1998) as:

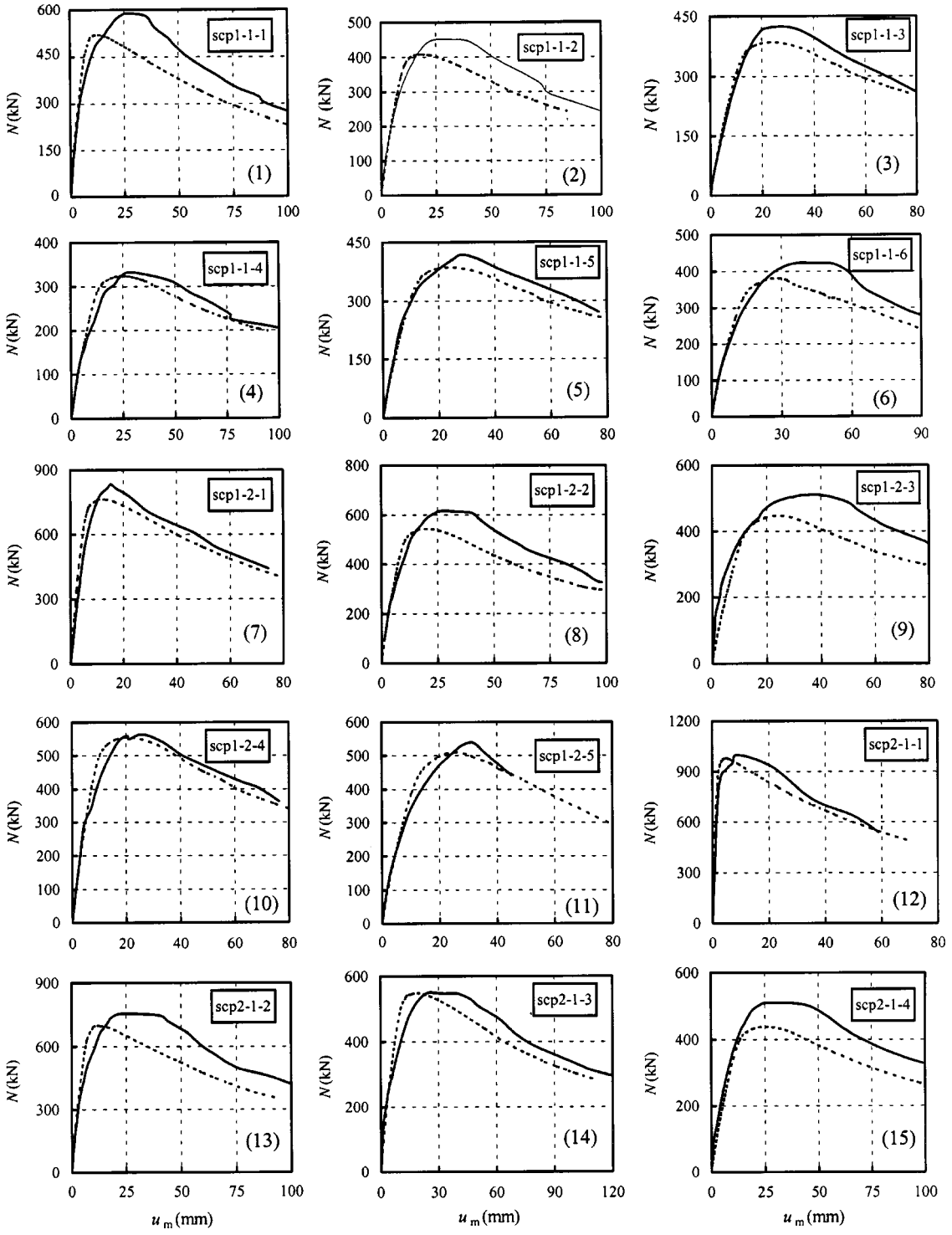

Fig. 5 Load versus mid-span lateral deflection curves(Experimental curves are shown in solid lines; Predicted curves are shown in dashed lines)

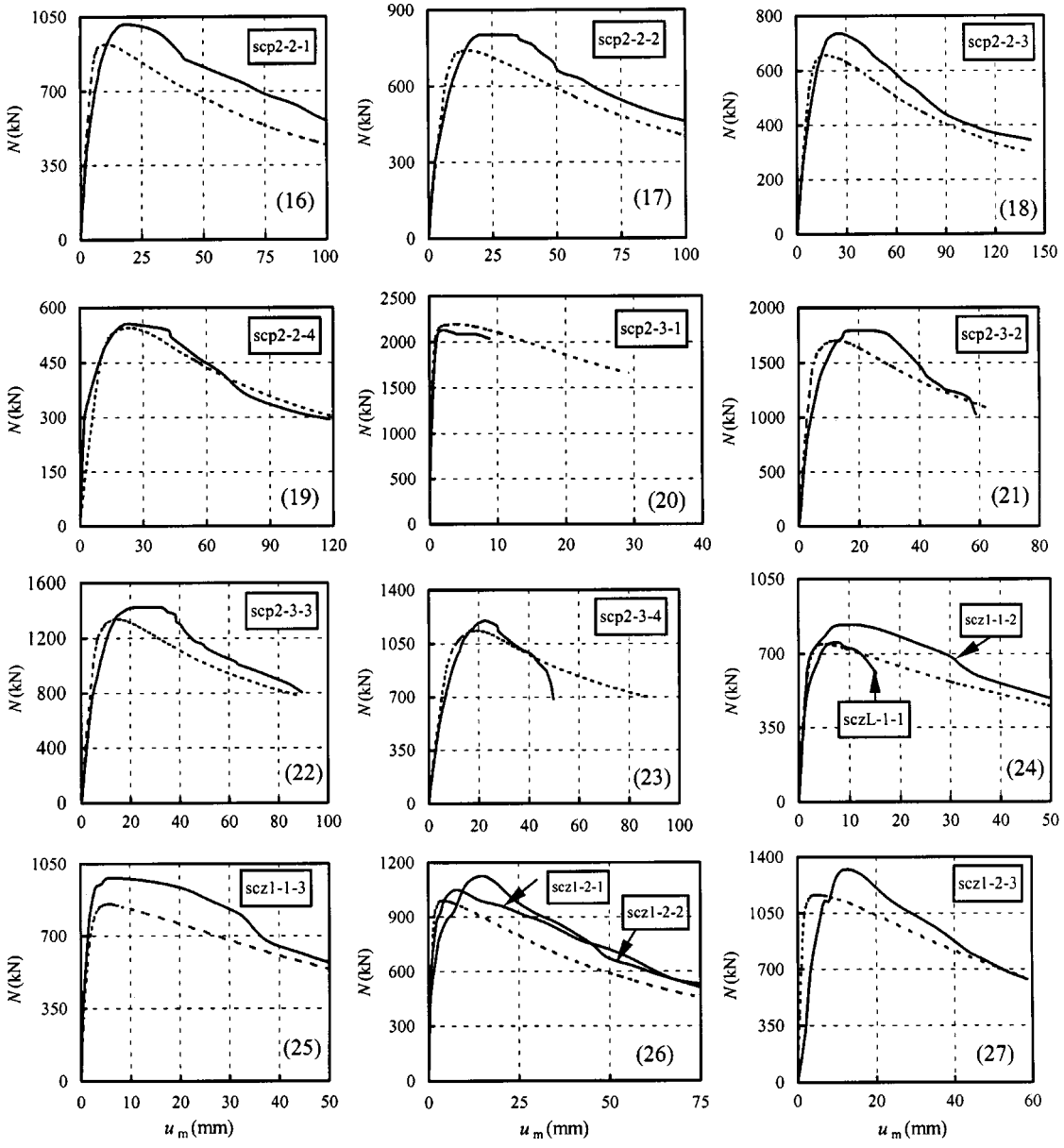

Fig. 5 Continued

$$\sigma = \sigma_o \cdot \left[A \cdot \left(\frac{\varepsilon}{\varepsilon_o} \right) - B \cdot \left(\frac{\varepsilon}{\varepsilon_o} \right)^2 \right] \qquad \text{for } \varepsilon \le \varepsilon_o \tag{6a}$$

$$\sigma = \sigma_o \cdot \left(\frac{\varepsilon}{\varepsilon_o} \right) \cdot \frac{1}{\beta \cdot \left(\frac{\varepsilon}{\varepsilon_o} - 1 \right)^{\eta} + \frac{\varepsilon}{\varepsilon_o}} \qquad \text{for } \varepsilon > \varepsilon_o \tag{6b}$$

in which

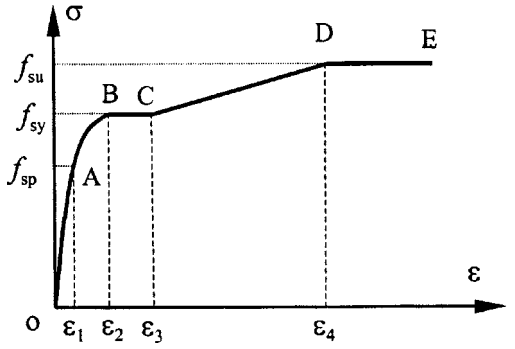

Fig. 6 Typical stress-strain curves for steel

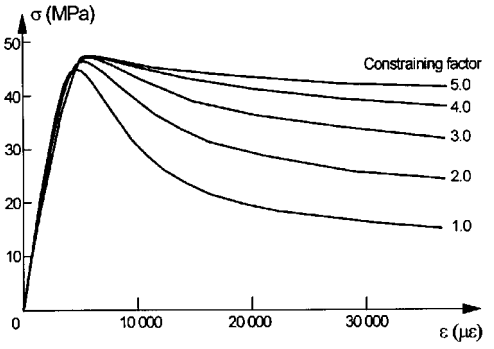

Fig. 7 Typical stress-strain curves for confined concrete

$$\sigma_o = f_{ck} \cdot \left[1.194 + 0.25 \cdot \left(\frac{13}{f_{ck}}\right)^{0.45} \cdot (-0.07845 \cdot \xi^2 + 0.5789 \cdot \xi)\right]$$

$$\varepsilon_o = \varepsilon_{cc} + 0.95 \cdot \left[1400 + 800 \cdot \left(\frac{f_{ck} - 20}{20}\right)\right] \cdot \xi^{0.2}, \quad \varepsilon_{cc} = 1300 + 14.93 \cdot f_{ck}$$

$$\eta = 1.60 + 1.5 \cdot \left(\frac{\varepsilon_o}{\varepsilon}\right), \quad A = 2.0 - k$$

$$B = 1.0 - k, \quad k = 0.1 \cdot \xi^{0.745}$$

$$\beta = \frac{0.75 \cdot f_{ck}^{0.1}}{\sqrt{1 + \xi}} \quad \text{for } \xi \le 3.0, \quad \beta = \frac{0.75 \cdot f_{ck}^{0.1}}{\sqrt{1 + \xi}(\xi - 2)^2} \quad \text{for } \xi > 3.0$$

The units for stress and strain are MPa and $\mu\varepsilon$ respectively.

It can be seen from Fig. 7 that the higher the confinement factor (ξ), the higher the compression strength of confined concrete. It can also be seen from Fig. 3 that the higher is ξ, the more ductile is the confined concrete. The confinement factor (ξ), to some extent, represents the composite action between steel tubes and concrete.

3.2. Load versus axial strain relations

The load versus axial strain relations can be established based on the following assumptions:

1. There is no slip between the steel and concrete
2. Longitudinal stress-strain models of steel and concrete are determined using the equations in Section 3.1
3. Force equilibrium and deformation consistencies are considered along the longitudinal direction, i.e.,

$$N = N_s + N_c \tag{7}$$

$$\varepsilon_{sl} = \varepsilon_{cl} \tag{8}$$

in which, N_s and N_c are forces carried by steel and concrete, ε_{sl} and ε_{cl} are longitudinal strains in steel and concrete.

The procedures to calculate load versus axial strain are expressed as:

For a given (ith) increment in axial strain $d\varepsilon_{li} \rightarrow i$th axial strain $\varepsilon_{l,i+1}=\varepsilon_{li}+d\varepsilon_{li} \rightarrow i$th axial stress $\sigma_{sl,i+1}$

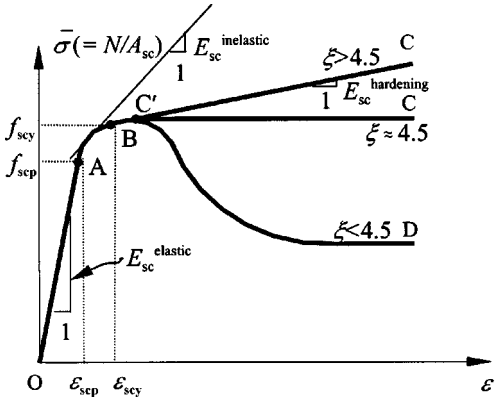

Fig. 8 Schematic view of combined stress-strain curves

and $\sigma_{cl,i+1} \rightarrow i$th forces $N_{s,i}$ and $N_{c,i} \rightarrow i$th force N_i or combined stress $\bar{\sigma}_i = N_i/A_{sc}$ where $A_{sc}=A_s+A_c$.

Typical curves of combined stress versus axial strain are shown schematically in Fig. 8. It can be seen that the curves are a function of the confinement factor (ξ). There are three or four stages in load versus axial curves, i.e.,

Stage 1: Elastic stage (from point O to point A). During this stage, steel and concrete bear load independently. The yielding of steel occurs at point A.

Stage 2: Elastic-plastic stage (from point A to point B). During this stage, concrete is confined by steel tube because the Poisson ratio of concrete is larger than that of steel. The confinement enhances as the longitudinal deformation increases.

Stage 3: Strain hardening stage (from point B to point C or from point B to point C'). During this stage, the load versus axial strain curves tend to go upwards. The shape of the curve depends on the value of confinement factor (ξ). When ξ is larger than 4.5, the curve goes up steadily to point C. When ξ is less than 4.5, the curve starts to go down after a short increase to point C'. The smaller the confinement factor, the earlier the curve starts to fall down.

Stage 4: Falling stage (from point C' to point D). This occurs only when the confinement factor (ξ) is less than 4.5. The smaller the confinement factor, the steeper the curve falls.

3.3. Load versus axial strain curves

The predicted curves of load versus axial strain (plotted in dashed lines) are compared in Fig. 2 and Fig. 9 with experimental curves. Good agreement is obtained between the predicted and tested curves.

3.4. Section capacity

The predicted section capacities ($N_{u,c}$) are compared in Table 1 with those obtained in tests ($N_{u,e}$). A mean ratio ($N_{u,e}/N_{u,c}$) of 1.006 is obtained with a COV (coefficient of variation) of 0.0491.

3.5. Simplified model

A series of combined stress ($\bar{\sigma}$) versus axial strain curves can be produced using the theoretical model described above. An example is shown in Fig. 10 for a range of confinement factors with

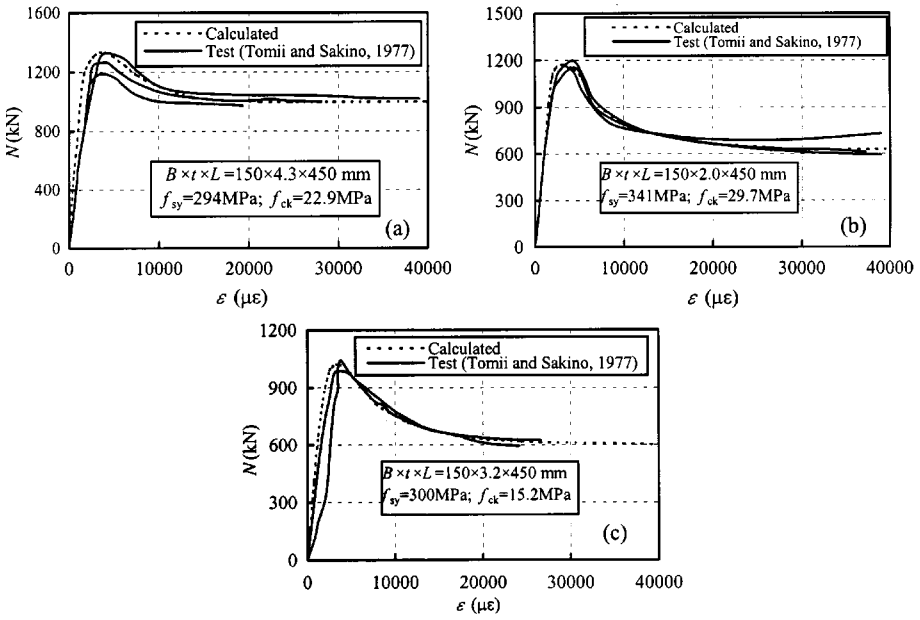

Fig. 9 Examples of comparisons: load versus axial strain curves (Experimental curves are shown in solid lines; Predicted curves are shown in dashed lines)

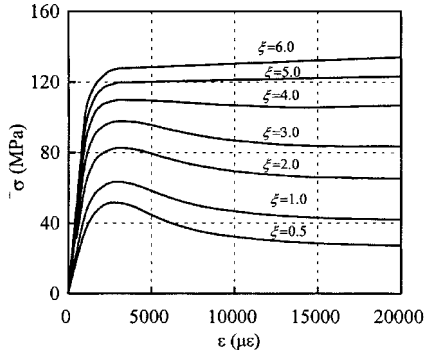

Fig. 10 Typical combined stress-strain curves

steel strength (f_{sy}) of 235 MPa and concrete strength (f_{ck}) of 32 MPa. Simplified models are established using regression analysis for section capacity and modulus in different stages.

3.5.1. Section capacity

The proposed model treats the composite section as one "material" with a total area of A_{sc}. The section capacity can be expressed as:

$$N_{uo} = f_{scy} \cdot A_{sc} \tag{9}$$

in which,

$$f_{scy} = (1.212 + B \cdot \xi + C \cdot \xi^2) \cdot f_{ck}, \quad B = 0.138 \cdot \frac{f_{sy}}{235} + 0.7646$$

$$C = -0.0727 \cdot \frac{f_{ck}}{20} + 0.0216, \quad A_{sc} = A_s + A_c$$

where the units for f_{sy} and f_{ck} are N/mm^2.

3.5.2. Modulus in different stages

The section modulus in different stages can be expressed as:

(1) Elastic stage

$$E_{sc}^{elastic} = \frac{f_{scp}}{\varepsilon_{scp}} \tag{10}$$

in which,

$$f_{scp} = \left(0.263 \cdot \frac{f_{sy}}{235} + 0.365 \cdot \frac{20}{f_{ck}} + 0.104\right) \cdot f_{scy}$$

$$\varepsilon_{scp} = 0.62 \cdot \frac{f_{sy}}{E_s}$$

in which, E_s is the Young's modulus of steel (taken as 200,000 MPa in this paper) and f_{scy} is given in Section 3.5.1.

(2) Inelastic stage

$$E_{sc}^{inelastic} = \frac{(f_{scp} - \sigma_{combined}) \cdot \sigma_{combined}}{(f_{scy} - f_{scp}) \cdot f_{scp}} \cdot E_{sc}^{elastic} \tag{11}$$

(3) Strain hardening (only for $\xi \geq 4.5$)

$$E_{sc}^{hardening} = 220 \cdot \xi + 450(\text{MPa}) \tag{12}$$

3.5.3. Comparison of section capacity

The section capacities predicted using the following four design methods are compared with the stub column test results obtained in the current tests and those from Cederwall *et al*. (1969), O'Shea and Bridge (1997) Song and Kwon (1997), Tomii and Sakino (1977), Tomii and Sakino (1979a), Tsuda and Matsui (1998), Kato (1995), Lu *et al*. (1999), Schneider (1998):

- LRFD (AISC 1994)
- AIJ (1997)
- Eurocode 4, part I (1996)
- The proposed method in this paper.

In all design calculations, the material partial safety factors were set to unity.

Predicted section capacities ($N_{u,c}$) using the different methods are compared with 101 experimental results ($N_{u,e}$) in Fig. 11(a)~(d). Table 3 shows both the mean value and the standard deviation (COV) of the ratio of $N_{u,c}/N_{u,e}$ for the different design methods. Results in this table clearly show that both LRFD, AIJ and EC4 are conservative. Overall, LRFD, AIJ and EC4 gave a section capacity about 10% lower than that of test. The proposed method predicted a slightly lower capacity than the test results. Overall, the proposed method adopting the concept of confinement factor gives a mean of 0.993 and a COV of 0.088, is the best predictor.

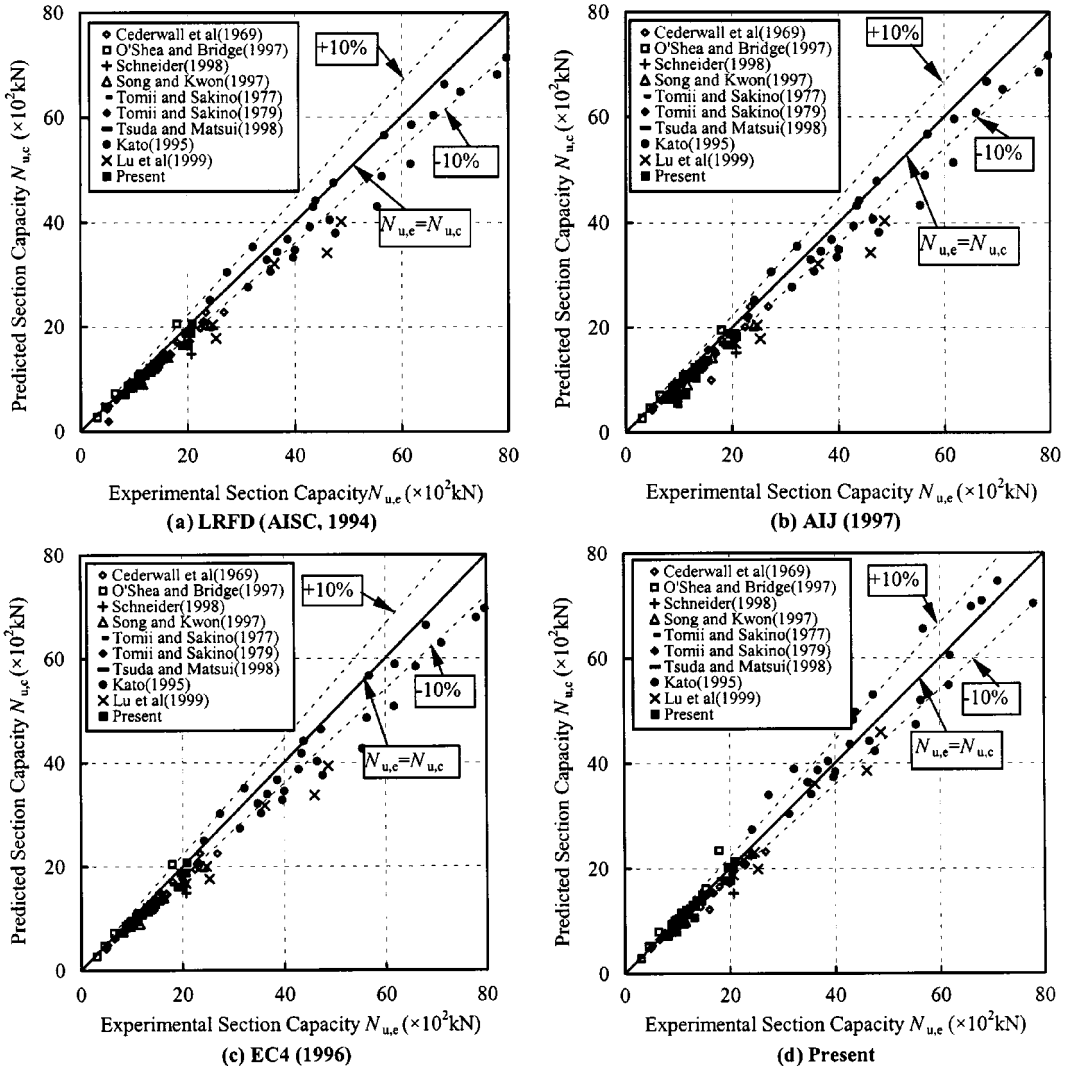

Fig. 11 Comparisons of section capacities

4. Mechanics model for concrete-filled SHS columns and beam-columns

4.1. Assumptions

A member subjected to compression is shown in Fig. 12 where N is the compression force, e is the load eccentricity and u_m is the mid-span deflection. When the load eccentricity (e) equals zero, the member under compression is called a column. Otherwise the member is called a beam-column, i.e., it is under combined bending and compression.

The load versus mid-span deflection relations can be established based on the following assumptions.

1. The stress-strain relationship for steel given in Eq. (4) is adopted for both tension and compression.
2. The stress-strain relationship for concrete given in Eq. (6) is adopted for compression only. The

Table 3 Comparisons between predicted section capacities and test results

No.	B (mm)	f_{ck} (MPa)	f_{sy} (MPa)	$N_{u,c}/N_{u,e}$ (LRFD, AISC 1994)		$N_{u,c}/N_{u,e}$ (AIJ 1997)		$N_{u,c}/N_{u,e}$ (EC41996)		$N_{u,c}/N_{u,e}$ (Present)		Speci-men num-ber	Test data resources
				Mean	COV	Mean	COV	Mean	COV	Mean	COV		
1	120	38.0-82.4	300.0-439.0	0.896	0.048	0.933	0.058	0.888	0.050	0.917	0.039	13	Cederwall, *et al.*(1969)
2	80-280	14.0-18.1	282.0	1.004	0.113	0.976	0.103	1.003	0.112	1.116	0.137	6	O'shea & Bridge(1997)
3	130-220	24.7	313.6	0.827	0.049	0.830	0.050	0.816	0.048	0.921	0.061	3	Song & Kwon (1997)
4	127	19.8-25	312-357	0.898	0.114	0.911	0.107	0.902	0.112	0.958	0.136	5	Schneider(1998)
5	150	15.2-29.7	294.0-341.0	0.911	0.026	0.914	0.026	0.903	0.028	1.009	0.031	9	Tomii & Sakino(1977)
6	100	16.6-26.2	194.0-339.1	0.820	0.190	0.894	0.032	0.886	0.038	0.975	0.018	8	Tomii & Sakino(1979)
7	150	25.9-27.3	288.1-357.7	0.917	0.023	0.922	0.023	0.905	0.018	1.020	0.045	5	Tsuda & Matsui(1998)
8	250	21.9-65.9	316.5-764.4	0.926	0.084	0.931	0.085	0.915	0.085	1.023	0.102	26	Kato(1995)
9	200-300	21.8-30.8	227.0	0.800	0.066	0.803	0.066	0.788	0.065	0.900	0.076	6	Lu *et al.*(1999)
10	120-200	12.2-36.6	321.1-331.1	0.921	0.042	0.927	0.038	0.917	0.044	0.997	0.047	20	Present
Total	80-300	12.2-82.4	194-764	0.904	0.092	0.917	0.071	0.902	0.074	0.993	0.088	101	--

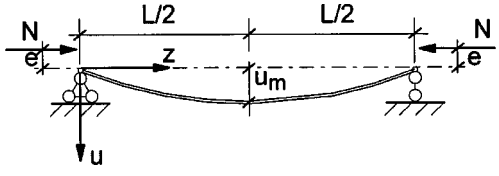

Fig. 12 A Schematic view of a beam-column

contribution of concrete in tension is neglected.

3. Original plane cross-sections remain plane.
4. The effect of shear force on deflection of members is omitted.
5. The deflection curve of the member is assumed as a sine wave.

4.2. Load versus mid-span deflection relations

According to the assumption No. 5, the deflection (u) of the member can be expressed as:

$$u = u_m \cdot \sin\left(\frac{\pi}{L} \cdot z\right) \tag{13}$$

where, u_m is the mid-span deflection, L is the length of the member and z is the horizontal distance from the left support as defined in Fig. 12.

The curvature (ϕ) at the mid-span can be calculated as:

$$\phi = \frac{\pi^2}{L^2} \cdot u_m \tag{14}$$

The strain distribution is shown in Fig. 13 where ε_o is the strain along the geometrical centre line of the section. The term ε_i is the strain at the location x_i as defined in Fig. 13. Along the line with $x = x_i$ the section can be divided into two elements (dA_{si} for steel and dA_{ci} for concrete) with unit depth. The strain at the centre of each element can be expressed as:

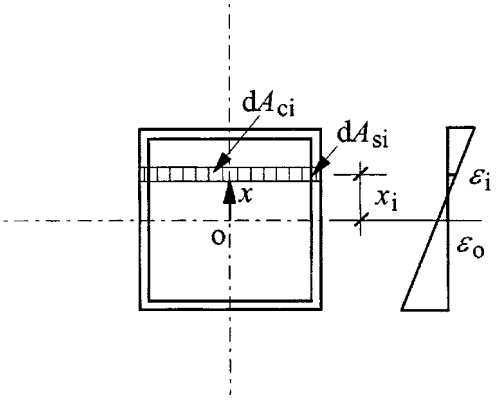

Fig. 13 Distribution of strains

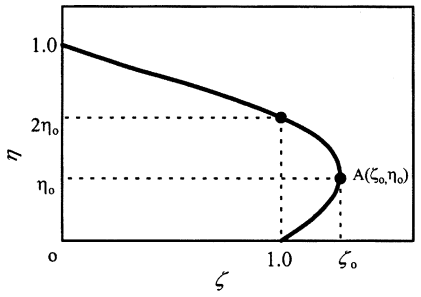

Fig. 14 A Schematic view of an interaction curve

$$\varepsilon_i = \varepsilon_o + \phi \cdot x_i \tag{15}$$

The stress at the centre of each element (σ_{si} for steel or σ_{ci} for concrete) can be determined using the stress-strain relationship given in Eq. (4) and Eq. (6). The internal moment (M_{in}) and axial force (N_{in}) can be calculated as:

$$M_{in} = \sum_{i=1}^{n} (\sigma_{si} \cdot x_i \cdot dA_{si} + \sigma_{ci} \cdot x_i \cdot dA_{ci}) \tag{16}$$

$$N_{in} = \sum_{i=1}^{n} (\sigma_{si} \cdot dA_{si} + \sigma_{ci} \cdot dA_{ci}) \tag{17}$$

According to the equilibrium condition,

$$M_{in} = M_{applied} \tag{18}$$

$$N_{in} = M_{applied} \tag{19}$$

From the above equations, the load versus mid-span deflection relations can be established for a certain eccentricity (e). The geometrical imperfection is taken as L/1000.

4.3. Comparison of member capacity and load-deflection relations

4.3.1. Member capacity of columns

The predicted column strengths are compared with the experimental values (see the last column in Table 2) where a mean of 1.072 and a COV (coefficient of variation) of 0.0682 are obtained.

4.3.2. load versus lateral deflection curves

The predicted curves of load versus lateral deflection (plotted in dashed lines) are compared in Fig. 5 with experimental curves. A good agreement is obtained between the predicted and tested curves.

4.3.3. Maximum loads in beam-columns

The predicted maximum strengths ($N_{u,c}$) are compared in Table 2 with those obtained in tests

($N_{u,e}$). A mean ratio ($N_{u,e}$/ $N_{u,c}$) of 1.084 is obtained with a COV of 0.0414.

4.4. Simplified model

4.4.1. Member capacity

The member capacity of columns (N_u) can be calculated using the section capacity with a stability reduction factor φ, i.e.,

$$N_u = \varphi \cdot N_{uo} \tag{20}$$

in which, is the sectional capacity, shown as in Eq. (9).

The stability reduction factor (φ) mainly depends on the slenderness ratio (λ), the yield stress of steel (f_{sy}), the compression strength of concrete (f_{ck}), the cross-section area ratio ($\alpha = A_s/A_c$). Simplified models are established based on regression analysis (Han 2000) for the stability reduction factor (φ), i.e.,

$$\varphi = 1.0 \qquad \text{for } \lambda \le \lambda_o \tag{21a}$$

$$\varphi = a \cdot \lambda^2 + b \cdot \lambda + c \qquad \text{for } \lambda_o < \lambda \le \lambda_p \tag{22b}$$

$$\varphi = \frac{d}{(\lambda + 35)^2} \qquad \text{for } \lambda > \lambda_p \tag{22c}$$

where

$$a = \frac{1 + (25 + 2 \cdot \lambda_p) \cdot g}{(\lambda_p - \lambda_o)^2}, \quad b = g - 2 \cdot a \cdot \lambda_p, \quad c = 1 - a \cdot \lambda_o^2 - b \cdot \lambda_o$$

$$d = \left(6300 + 7200 \cdot \frac{235}{f_{sy}}\right) \cdot \left(\frac{25}{f_{ck} + 5}\right)^{0.3} \cdot \left(\frac{A_s}{0.1 \cdot A_c}\right)^{0.1}, \quad g = \frac{-d}{(\lambda_p + 35)^2}$$

$$\lambda_o = \pi \cdot \sqrt{\frac{220 \cdot \xi + 450}{f_{scy}}} \tag{23}$$

$$\lambda_p = \pi \cdot \sqrt{\frac{E_s}{0.62 \cdot f_{sy}}} \tag{24}$$

in which E_s is the Young's modulus of steel (taken as 200,000 MPa in this paper) and f_{scy} is given in Eq. (9).

4.4.2. Interaction curves

Simplified models are established based on regression analysis (Han 2000) for interaction relationship between compression strength and bending strength. A schematic view of an interaction curve is shown in Fig. 14.

The horizontal axis refers to the ratio (η) of applied moment (M) to the moment section capacity (M_u) under pure bending. The calculation of the moment capacity (M_u) is not covered in this paper. Mechanics model for M_u can be found in Zhao and Grzebieta (1999). The vertical axis refers to the ratio of applied compression force (N) to the section capacity (N_u). The coordinates of the contraflexure point A (η_o , ζ_o) in Fig. 14 can be calculated as:

$$\eta_o = 0.201 \cdot \left(\frac{f_{ck}}{20}\right)^{0.65} \cdot \left(\frac{235}{f_{sy}}\right)^{0.38} \cdot \left(\frac{0.1 \cdot A_c}{A_s}\right)^{0.45} \tag{25}$$

$$\zeta_o = 1.0 + 0.113 \cdot \left(\frac{f_{ck}}{20}\right)^{1.46} \cdot \left(\frac{235}{f_{sy}}\right)^{1.65} \cdot \left(\frac{0.1 \cdot A_c}{A_s}\right)^{1.4} \tag{26}$$

The interaction curve can be expressed as:

$$\frac{\zeta}{1 - 0.25N/N_E} = \begin{cases} \dfrac{1 - \eta/\varphi}{1 - 2\eta'_o/\varphi} & \text{for} \quad \eta \geq 2\eta'_o \\ a\left(\dfrac{\eta}{\varphi}\right)^2 + b\left(\dfrac{\eta}{\varphi}\right) + 1 & \text{for} \quad \eta < 2\eta'_o \end{cases}$$

where

$N_E = \pi^2 E_{sc}^{elastic} A_{sc}/\lambda^2$, $E_{sc}^{elastic}$ is the section modulus of concrete filled SHS in elastic stages;

$\eta'_o = \varphi^3 \eta_o$; $\zeta'_o = 1 + \varphi^5(\zeta_o - 1)$; $a = (1 - \zeta'_o)/\eta'^2_o$; $b = -2\eta'_o(1 - \zeta'_o)/\varphi\eta'_o$

4.4.3. Comparison

The predicted interaction curves (M/M_u-N/N_u) using the proposed method are compared in Fig. 15 with the experimental values from the current tests. Good agreement is achieved.

The member capacities predicted using the following four design methods are compared with the columns and beam-columns test results those obtained in the current tests and those from Matusi *et al.* (1997), Cederwall *et al.* (1969), Furlong (1967), Knowles and Park (1969), Nakamura (1994), O'Shea and Bridge (1997), Schneider (1998), Song and Kwon (1997), Tomii and Sakino (1977), Tomii and Sakino (1979a), Tsuda and Matsui (1998), Kato (1995), Lu *et al*. (1999), Zhang (1989), Zhang (1993), Tomii and Sakino (1979b), Bridge (1976), Uy (1997), Li *et al*. (1998):

- LRFD (AISC 1994)
- AIJ (1997)
- Eurocode 4, part I (1996)
- The proposed method in this paper.

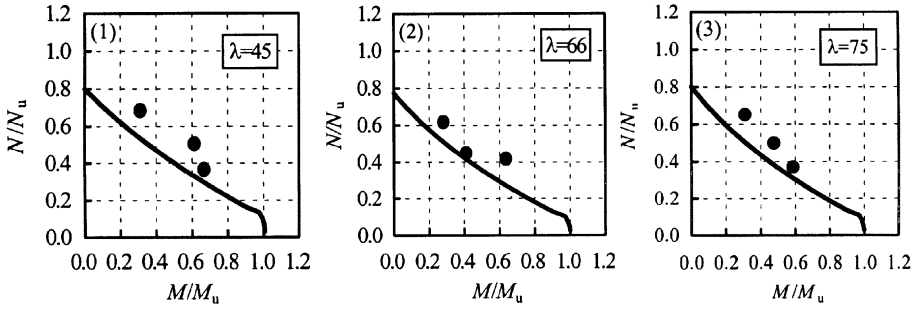

Fig. 15 Comparison of predicted interaction curves with test results by the authors

Table 4 Comparison between predicted member capacities and test results

No.	B (mm)	t (mm)	f_{sy} (MPa)	f_{ck} (MPa)	λ	e (mm)	$N_{u,c}/N_{u,e}$								Specimen Number	Test Resources
							LRFD (1994)		AIJ (1997)		EC4 (1996)		Present			
							Mean	COV	Mean	COV	Mean	COV	Mean	COV		
1	150	4.3	412	26	14-104	0-125	0.944	0.133	0.857	0.077	0.899	0.053	1.034	0.060	24	Matusi *et al.*(1997)
2	120	5-8	300-439	38-82	14-87	0-20	0.957	0.082	0.822	0.126	0.862	0.054	0.930	0.061	28	Cederwall *et al.*(1969)
3	102-127	2.1-4.8	331-485	20-36	14-31	0-466	0.787	0.115	0.909	0.02	0.985	0.113	0.964	0.106	21	Furlong(1967)
4	76	3.4	324	33	12-79	0-25	1.026	0.096	0.971	0.153	1.016	0.065	1.058	0.102	10	Knowles & Park(1969)
5	60	1.5	431	20-22	14-101	0	0.943	0.031	0.830	0.098	0.950	0.039	1.010	0.054	7	Nakamura(1994)
6	80-280	2.1	282	14-18	12	0	1.004	0.113	0.976	0.103	1.003	0.112	1.116	0.137	6	O'shea & Bridge(1997)
7	127	3.2-7.5	312-357	20-25	17	0	0.898	0.114	0.911	0.107	0.902	0.112	0.958	0.136	5	Schneider(1998)
8	130-220	3.0-3.2	314	25	10	0	0.827	0.049	0.830	0.050	0.816	0.048	0.921	0.061	3	Song & Kwon(1997)
9	150	2.0-4.3	294-341	15-30	10	0	0.911	0.026	0.914	0.026	0.903	0.028	1.009	0.031	9	Tomii & Sakino(1977)
10	100	2.2-4.3	194-339	17-26	10	0	0.820	0.190	0.894	0.032	0.886	0.038	0.975	0.018	8	Tomii &Sakino(1979a)
11	150	1.6-5.6	288-358	26-27	10	0	0.917	0.023	0.922	0.023	0.905	0.018	1.020	0.045	5	Tsuda & Matsui(1998)
12	200-250	4.5-12	317-764	22-66	10	0	0.926	0.084	0.931	0.085	0.915	0.085	1.023	0.102	26	Kato(1995)
13	200-300	5.0	227	22-31	10	0	0.800	0.066	0.803	0.066	0.788	0.065	0.900	0.076	6	Lu *et al.*(1999)
14	150	2.0-6.9	218-292	22-34	29-101	0	0.911	0.062	0.710	0.149	0.910	0.063	0.912	0.079	30	Zhang(1993)
15	100	2.2-4.3	194-339	15.6-31.2	10	25-308	0.680	0.108	0.882	0.062	1.003	0.191	0.937	0.051	24	Tomii &Sakino(1979b)
16	152-204	6.5-10	290-319	24.6-36.0	36-69	38-64	0.995	0.042	0.961	0.086	0.962	0.028	1.058	0.053	8	Bridge(1976)
17	126-186	3.0	300	26.2-40.3	17	20-84	0.642	0.203	0.830	0.088	0.839	0.091	0.878	0.121	8	Uy(1997)
18	150-152	3.0-8.3	242-308	21.7-28.5	14-59	0.6-75	0.824	0.161	0.862	0.127	0.888	0.126	0.949	0.135	16	Li *et al.*(1998)
19	149-200	3.9-7.8	205-300	33.8	18-24	30-120	0.678	0.080	0.919	0.152	0.908	0.148	0.951	0.131	18	Zhang(1989)
20	120-200	3.8-5.9	321-330	18-37	45-75	0-80	0.884	0.063	0.829	0.116	0.857	0.077	0.943	0.072	29	Present
Total	60-300	1.5-12	194-764	14-82	10-104	0-466	0.858	0.140	0.853	0.126	0.898	0.114	0.957	0.104	331	--

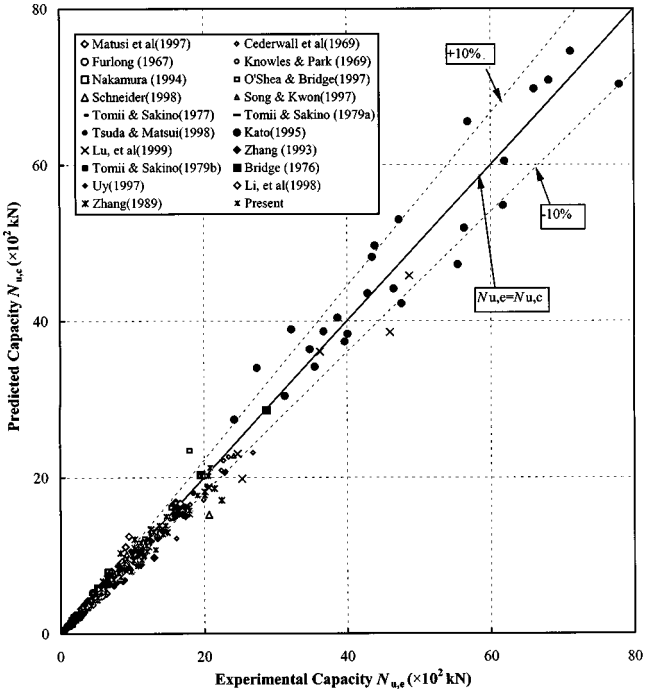

Fig. 16 Comparison of maximum loads in beam-columns

In all design calculations, the material partial safety factors were set to unity.

Predicted section capacities ($N_{u,c}$) using the different methods are compared with 331 experimental results ($N_{u,e}$). Table 4 shows both the mean value and the standard deviation (COV) of the ratio of $N_{u,c}/N_{u,e}$ for the different design methods. Results in this table clearly show that the LRFD, AIJ and EC4 are conservative. Overall, LRFD, AIJ and EC4 gave a member capacity about 10% lower than that of test. The proposed method predicted a slightly lower capacity than the test results. Overall, the proposed method with a mean of 0.957 and a COV of 0.104, is the best predictor. Fig. 16 shows the comparison between the predicted section capacities ($N_{u,c}$) by using the proposed method and those experimental results ($N_{u,e}$).

The predicted interaction curves (M_u-N_u) using the different methods are compared in Fig. 17 with the a set of experimental values obtained by Matsui *et al*. (1997), parameters of the sections of the tested members were as followings: $B\times t$ = 149.8×4.27 mm; f_{sy}=411.6 MPa and f_{ck}=25.4 MPa. Slenderness ratios were shown in the figures.

5. Conclusions

Twenty stub column tests, eight column tests and twenty-one beam-column tests have been performed on concrete-filled square hollow sections. Mechanics models have been established for concrete-filled SHS stub columns, columns and beam-columns. A confinement factor has been used to describe the composite action between steel tubes and concrete. The following observations and conclusions are made based on the limited research reported in the paper.

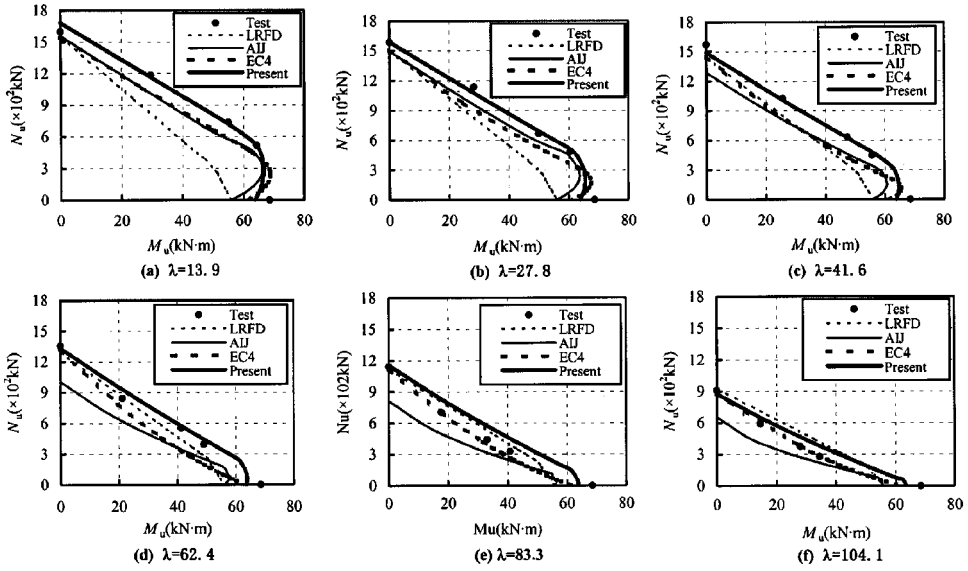

Fig. 17 Comparison of predicted interaction curves with test results by the Matsui *et al.* (1997)

(1) The section ductility increases significantly when the constraining factor exceeds 3.5.

(2) The load versus axial strain relationship has been established for concrete-filled SHS stub columns. A good agreement in load versus axial strain relationship and in section capacities has been obtained between the predicted and experimental values.

(3) Simplified models have been developed to estimate the section capacity and section modulus. The predicted section capacity has been compared with that of 101 experimental results with a wide range of parameters such as the confinement factor (ξ), the concrete strength (f_{ck}) and the steel yield stress (f_{sy}). Overall, the proposed method adopting the concept of confinement factor agrees well with test results and existing codes.

(4) The predicted load versus lateral deflection curves have been found in good agreement with experimental values. The predicted maximum strength of beam-columns agrees well with the tested values.

(5) A simplified model has been proposed for interaction curves of compression and bending. The predicted column and beam-column strength has been compared with that of 331 column tests with a wide range of parameters such as the confinement factor (ξ), the slenderness ratio (λ), the concrete strength (f_{ck}), the steel yield stress (f_{sy}) and the load eccentricities (e). A good agreement has been obtained. Overall, the proposed method adopting the concept of confinement factor agrees well with test results.

References

ASCCS (1997), "Concrete filled steel tubes - a comparison of international codes and practices", ASCCS Seminar, Innsbruck, September.

AISC (1994), "Load and resistance factor design specification for structural steel buildings", American Institute of Steel Construction, Inc., Chicago, September.

Architectural Institute of Japan (AIJ) (1997), "Recommendations for design and construction of concrete filled steel tubular structures", Oct.

Bergmann, R. *et al*. (1995), "Design guide for concrete-filled hollow section columns under static and seismic loading", CIDECT, Verlag TUV Rheinland GmbH, Köln, Germany.

Bridge, R.Q., O'Shea, M.D., Gardener, P., Grigson, R. and Tyrell, J. (1995), "Local buckling of square thin-walled steel tubes with concrete infill", in *Structural Stability and Design*, Kitiporchai, Hancock, Bradford (eds), Balkema, Rotterdam, The Netherlands, 307-314.

Bridge, R.Q. (1976). "Concrete filled steel tubular columns", *Civil Engineering Transactions*, 127-133.

Cederwall, K., Engstrom, B. and Grauers, M. (1969), "High-strength concrete used in composite columns", *High-Strength Concrete*, SP121-11, 195-210.

Eurocode 4. (1996), "Design of steel and concrete structures, Part1. 1,General rules and rules doe building", DD ENV 1994-1-1: British Standards Institution, London W1A2BS.

Furlong, R.W. (1967), "Strength of steel-encased concrete beam-columns", *J. Struct. Engrg*., ASCE, **93**(5), 113-124.

Ge, H.B. and Usami, T. (1992), "Strength of concrete-filled thin-walled steel box columns: Experiment", *Journal of Structural Engineering*, ASCE, **118**(11), 3006-3054.

Ge, H. B. and Usami, T. (1994), "Strength analysis of concrete-filled thin-walled steel box columns", *Journal of Constructional Steel Research*, **30**, 607-612.

Ge, H. B. and Usami, T. (1996), "Cyclic tests of concrete filled steel box columns", *Journal of Structural Engineering*, ASCE, **122**(10), 1169-1177.

Han, L.H.(1998), "Fire resistance of concrete filled steel tubular columns", *Advances in Structural Engineering An International Journal*, **2**(1), 35-39.

Han, L. H. (2000), "Concrete filled steel tubular structures", Peking, Science Press (in Chinese).

Kato, B. (1995), "Compressive behaviors of concrete filled steel stub columns", *Transactions of A.I. J*., No. 468, 183-191 (in Japanese).

Kitada, T. (1998), "Ultimate strength and ductility of state-of-the-art concrete-filled steel bridge piers in Japan", *Engineering Structures*, **20**(4-6), 347-354.

Knowles, R.B. and Park, R. (1969), "Strength of concrete filled steel tubular columns", *J. Struct. Engrg*., ASCE, **95**(12), 2565-2587.

Li, S.P., Huo, D., Wang, Q., Guo, Y.C. and Huang, Y.Y. (1998), "Compression strengths of concrete-filled SHS columns", *Journal of Constructional Structures*, Issue No. 2, 41-51 (in Chinese).

Liu, Z.Y. and Goel, S. (1988), "Cyclic load behaviour of concrete-filled tubular braces", *Journal of Structural Engineering*, ASCE, **114**(7), 1488-1506.

Lu, X.L., Yu, Y. and Chen, Y.Y. (1999), "Tests on the behavior of concrete filled steel tubes subjected to axial compression", *Building Construction*, No. 10, 41-43 (in Chinese).

Mander, J.B., Priestley, M.J.N. and Park, R. (1988a), "Theoretical stress-strain model for confined concrete", *Journal of Structural Engineering*, ASCE, **114**(8), 1804-1826.

Mander, J.B., Priestley, M.J.N. and Park, R. (1988b), "Observed stress-strain behaviour of confined concrete", *Journal of Structural Engineering*, ASCE, **114**(8), 1827-1849.

Murray, N.W. (1986), "Introduction to the theory of thin-walled structures", *Clarendon Press*, Oxford, UK.

Matsui, C., Mitani, I., Kawano, A. and Tsuda, K. (1997), "AIJ design method for concrete filled tubular structures", ASCCS Seminar, September, Innsbruck, 93-116.

Nakai, *et al*. (1986), "An analysis on ultimate strength of concrete filled rectangular steel tubular columns subjected to compression and bending", *Proceedings*, *Civil Engineering*, No. 374 (I-6), October, 447-456 (in Japanese).

Nakai, *et al*. (1994), "Experimental study on ultimate strength and ductility of concrete filled thin-walled steel box columns after receiving seismic loading", *J. Structural Engineering*, JSCE, 40A, 1401-1412 (in Japanese).

Nakamura, T. (1994), "Experimental study on compression strength of concrete-filled square tubular steel columns", *J. Struct. Engrg*, 40B, 411-417.

O'shea, M. and Bridge, R.Q. (1997), "The design for local buckling of concrete filled steel tubes", *ASCCS Seminar*, September, Innsbruck, Austria, 319-324.

Pan, Y.G. (1988), "Analysis of complete curve of concrete filled steel tubular stub columns under axial compression", *Proc. of International Conference on Concrete Filled Steel Tubular Structures(including Composite Beams)*, Harbin, P. R. China, 87-93.

SAA. (1996), Cold-Formed Steel Structures, Australian/New Zealand Standards AS/NZS 4600, Standards Australia, Sydney, Australia.

Shams, M. and Saadeghvaziri, M.A. (1997), "State of the art of concrete-filled steel tubular columns", ACI *Structural Journal*, **94**(5), 558-571.

Schneider, S.P. (1998), "Axially loaded concrete-filled steel tubes", *Journal of Structural Engineering*, ASCE, **124**(10), 1125-1138.

Song, J.Y. and Kwon, Y.B. (1997), "Structural behavior of concrete-filled steel box sections", *Int. Confer. Report on Composite Construction-Conventional and Innovative*, Innsbruck, Austria, 795-801.

Tao, Z., Han, L.H. and Zhao, X.L. (1998), "Behaviour of square concrete filled steel tubes subjected to axial compression", *Proceedings of The Fifth International Conference on Structural Engineering for Young Experts*, Shenyang, P.R. China, 61-67.

Tomii, M. and Sakino, K. (1977), "Experimental study of concrete filled steel tubular stub columns under concentric loading", *Proc. of the Int. Colloquium on Stability Of Structures under Static and Dynamic Loads*, SSRC/ASCE/Washington, D.C./ March 17-19, 718-741.

Tomii, M. and Sakino, K. (1979a), "Experimental studies on the ultimate moment of concrete filled square steel tubular beam-columns", *Trans. of A.I.J.* No. 275, Jan. 55-63.

Tomii, M. and Sakino, K. (1979b), "Elasto-plastic behavior of concrete filled square steel tubular beam-columns", *Trans. Of A.I. J,* No. 280 (June), Tokyo, Japan, 111-120.

Trezona, J.R. and Warner, R.F. (1997), "Strength of concrete-filled circular steel tubular columns", Research Report No. R147, January, Department of Civil and Environment Engineering, The University of Adelaide, Adelaide.

Tsuda, K., Matsui, C. (1998), "Limitation on width (Diameter)-thickness ratio of steel tubes of composite tubes and concrete columns with encased type section", *Proc. of Fifth Pacific Structural Steel Conf.,* Seoul, Korea, 865-870.

Uy, B. (1997), "Ductility and strength of thin-walled concrete filled box columns," *Int. Confer. Report on Composite Construction-Conventional and Innovative*. Innsbruck, Austria, 801-806.

Uy, B. (1998), "Local and post-local buckling of concrete filled steel welded box columns", *Journal of Constructional Steel Research,* **47**, 47-72.

Uy, B., Wright, H.D. and Diedricks, A.A. (1998), "Local buckling of cold-formed steel sections filled with concrete", *Proc., 2nd International Conference on Thin-Walled Structures*, Singapore, 367-374

Zhang, Z.G. (1989), "Behaviour of concrete-filled SHS beam-columns", *Constructional Structures*, Issue No. 6, 10-20 (in Chinese).

Zhang, Z.G. (1993), "Stability analysis of concrete-filled shs slender columns", *Journal of Constructional Structures*, Issue No. 8, 28-390 (in Chinese).

Zhao, X.L. and Grzebieta, R.H. (1999), "Void-filled SHS beams subjected to large deformation cyclic bending", *Journal of Structural Engineering*, ASCE, **125**(9), 1020-1027.

Zhao, X.L., Grzebieta, R.H., Wong, P. and Lee, C. (1999), "Void-filled RHS sections subjected to cyclic axial tension and compression", *Advances in Steel Structures*, Chan and Teng (eds), Elsevier, **1**, 429-436.

Zhao, X.L. and Hancock, G.J. (1991), "Tests to determine plate slenderness limits for cold-formed rectangular hollow sections of grade C450", *Steel Construction*, Australian Institute of Steel Construction, **25**(4), 2-16.